Distributed feedback quantum cascade lasers operating in continuous-wave mode at $\lambda \approx 7.6\ \mu$m*

Zhang Jinchuan(张锦川)[1,2], Wang Lijun(王利军)[1,†], Liu Wanfeng(刘万峰)[1], Liu Fengqi(刘峰奇)[1], Zhao Lihua(赵立华)[1], Zhai Shenqiang(翟慎强)[1], Liu Junqi(刘俊岐)[1], and Wang Zhanguo(王占国)[1]

[1]Key Laboratory of Semiconductor Materials Science, Institute of Semiconductors, Chinese Academy of Sciences, Beijing 100083, China
[2]Department of Electronic Engineering, Tsinghua University, Beijing 100084, China

Abstract: Distributed feedback (DFB) quantum cascade lasers (QCLs) in continuous-wave (CW) mode emitting at $\lambda \approx 7.6\ \mu$m are presented. Holographic lithography was used to fabricate the first-order distributed feedback grating. For a high-reflectivity-coated QCL with 14.5-μm-wide and 3-mm-long cavity, CW output powers of 300 mW at 85 K and still 10 mW at 270 K are obtained. Single-mode emission with a side-mode suppression ratio (SMSR) of about 30 dB and a wide tuning range of ~300 nm in the temperature range from 85 to 280 K is observed.

Key words: quantum cascade laser; distributed feedback; holographic lithography
DOI: 10.1088/1674-4926/33/2/024005 **PACC:** 4260F; 3320E; 4240E

1. Introduction

The quantum cascade laser (QCL) is currently one of the most flexible and powerful light sources for many chemical sensing applications in the mid-infrared region of the spectrum such as gas sensing, military countermeasures, medical diagnosis and free space communication[1−5]. The realization of these applications is fulfilled only with the employment of distributed feedback (DFB) QCLs operating in CW mode which have a single-mode, very narrow spectral linewidth and wide tuning range. However, the gratings of these devices are usually fabricated by electron-beam lithography, which is particularly expensive and time-consuming. As the commercial significance of QCLs increases, the production of reliable and potentially low cost devices becomes increasingly important. Thus, holographic lithography technique for its high efficiency and low cost has been demonstrated to realize CW operation, single-mode QCLs[6−8]. Unfortunately, the emitting wavelength of DFB-QCLs are mainly concentrated on the first atmospheric window (3–5 μm) due to the lack of good CW Fabry–Pérot (F–P) QCLs in the range of wavelength $\lambda > 7\ \mu$m. At present, there are very few groups who can achieve room temperature CW operation of DFB-QCLs in this wavelength range[9−11] and electron-beam lithography seems indispensable for the fabrication of gratings. For practical reasons, the use of holographic lithography technique to pattern the grating should be remarkable. In this letter, we applied the holographic lithography technique to the fabrication of DFB-QCLs at $\lambda \approx 7.6\ \mu$m. This QCL wavelength is rather attractive because it targets the common industrial pollutant molecules, such as SO_2 and CH_4. Single-mode emission with a high side-mode suppression ratio (SMSR) and a wide tuning range is achieved up to a temperature of 280 K.

2. Device structure and fabrication

The quantum cascade laser structure was grown by solid-source molecular beam epitaxy on an n-InP (Si, 3×10^{17} cm^{-3}) substrate in a single epitaxial run. A 1.55 μm active region was sandwiched between two 300-nm-thick InGaAs layers. The first-order DFB grating of periodicity $\Lambda = 1.192\ \mu$m (duty cycle of ~ 65%) was designed on the upper 300 nm-thick InGaAs layer using the holographic lithography technique and subsequently etched to a depth of about 90 nm by wet chemical etching. Then 3 μm thick low-doped (2.4×10^{16} cm^{-3}) InP layer and a 0.5 μm thick high-doped (5×10^{18} cm^{-3}) InP layer were grown in sequence as the upper cladding by metal-organic chemical-vapor deposition (MOCVD). A target wavelength of $\lambda = 7.58\ \mu$m is chosen based on the emission spectra of the F–P lasers. The scanning electron microscope (SEM) image of the cross section of DFB-QCL structure is shown in Fig. 1.

Following implementation of the grating pattern and regrowth, the epi-wafer was etched into double-channel waveguide laser with an average ridge width of 14.5 μm. The ridge structures were passivated with insulating layers of SiO_2 with thickness around 350 nm deposited by chemical vapor deposition. The devices were then fabricated with e-beam evaporated Ti/Au layer, followed by a 5.5-μm-thick electroplated gold layer, and thinned down to about 120 μm total thickness. Ge/Au/Ni/Au metal was used as substrate contact layer and the processed wafer were cleaved to a length of 3-mm bars and a high-reflectivity coating consisting of Al_2O_3/Ti/Au/Ti/Al_2O_3

* Project supported by the National Science Fund for Distinguished Young Scholars of China (No. 60525406), the National Natural Science Foundation of China (Nos. 60736031, 60806018, 60906026), and the National High Technology Research and Development Program of China (Nos. 2007AA03Z446, 2009AA03Z403).
† Corresponding author. Email: ljwang@semi.ac.cn
Received 15 August 2011

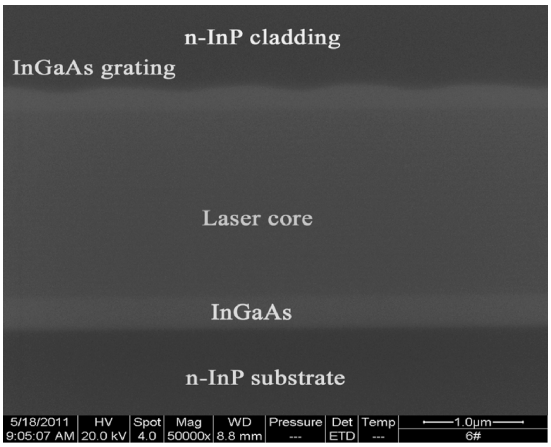

Fig. 1. SEM image of the cross-sectional view of DFB-QCL structure.

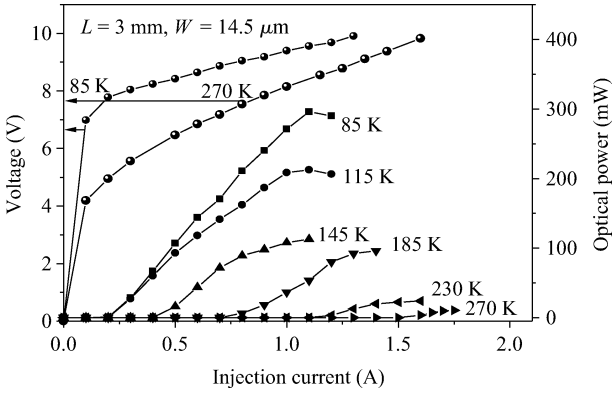

Fig. 2. Output power versus current of a 3-mm-long and 14.5-μm-wide DFB laser operated in CW mode at different heat sink temperatures between 85 K and 270 K along with V–I curves at 85 K and 270 K.

(200/10/100/10/120 nm) was deposited on the back facet.

The lasers were mounted epilayer-side down on copper heat sinks with indium solder and then wire bonded to an external contact pad. For low temperature testing, the lasers were mounted inside a liquid nitrogen cooled cryostat. The emitted optical power from the facet of lasers was measured with a calibrated thermopile detector placed directly in front of the laser facet.

3. Measurement and results

Figure 2 shows the CW operation power–current–voltage (P–I–V) characteristics of the DFB device with a 14.5-μm-wide and 3-mm-long cavity at different heat sink temperatures (85–270 K). A high output power of 300 mW is obtained at 85 K with a threshold current density ($J_{\rm th}$) of 0.41 kA/cm^2 and the output power decreased to 10 mW with $J_{\rm th} = 3.45$ kA/cm^2 at 270 K. The voltage–current (V–I) curves at both 85 and 270 K are also shown in Fig. 2. The threshold voltage ($V_{\rm th}$) of 7.7–9.6 V was measured over the temperature range of 85–270 K.

Figure 3 shows the normalized CW emission spectra (in semilog scale) of the same DFB laser obtained at currents of $1.1I_{\rm th}$ for the temperature range of 85–280 K. Single-mode

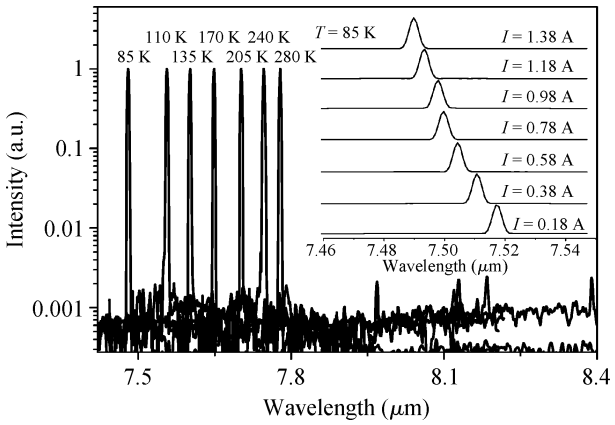

Fig. 3. Single-mode CW emission spectra of a DFB laser at currents of $1.1I_{\rm th}$ for different heat sink temperatures of 85–280 K. The inset shows the lasing frequency change at different driving currents at a constant temperature of 85 K.

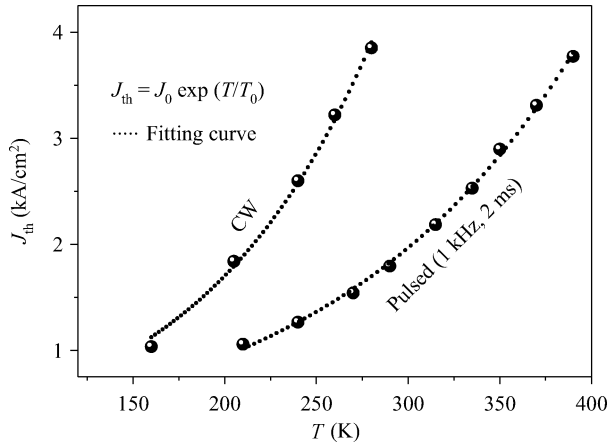

Fig. 4. Threshold current as a function of heat sink temperature in CW and pulsed modes of a 3-mm-long and 14.5-μm-wide DFB laser. The dotted line is the fitting result using a usual exponential function $J_{\rm th} = J_0 \exp(T/T_0)$.

emission with a SMSR about 30 dB in all tested temperature range is observed. The spectra were measured by using a Fourier transform infrared (FTIR) spectrometer with a 0.5 cm^{-1} resolution. The peak emission was observed to shift from 7.478 μm at 85 K to 7.778 μm at 280 K corresponding to a tuning range of 300 nm. The inset of Fig. 3 shows the normalized CW emission spectra, obtained at different currents from 0.18 to 1.38 A with a step of 0.2 A at 85 K. Single-mode emission in the entire current range is observed.

The temperature rise of active region during CW operation is obvious though the lasers were mounted epilayer-side down on copper heat sinks. Usually, the active region temperature $T_{\rm act}$ is much higher than the heat sink temperature $T_{\rm sink}$ in CW mode. The measured the threshold current density as the function of heat sink temperature in CW and pulsed modes is shown in Fig. 4. In pulsed mode, a 2 μs pulse width with a repetition rate of 1 kHz was used. Fitting the experimental result with the expression $J_{\rm th} = J_0 \exp(T/T_0)$ gives a characteristic temperature of $T_0 = 137$ K in pulsed mode and $T_0 = 100$ K in CW mode.

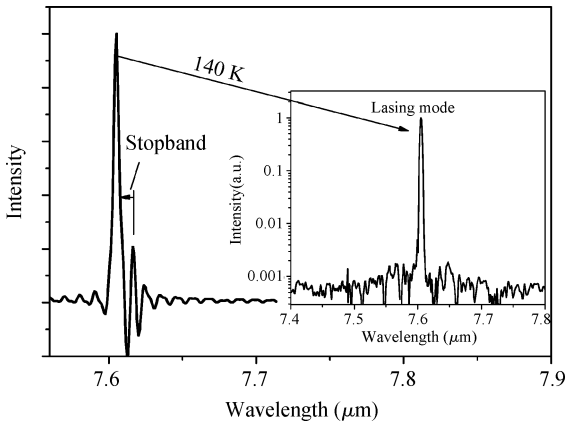

Fig. 5. Subthreshold CW emission spectrum at 140 K with injection current of 0.318 A. The inset is the lasing spectrum at the injection current of 0.32 A.

The actual core temperature of the laser is approximately equal to the heat sink temperature measured in pulsed mode at low duty cycles, where heating effects are negligible. At 270 K, the thermal resistance of the laser, which is defined as $R_{\rm th} = (T_{\rm act} - T_{\rm sink})/(V_{\rm th} I_{\rm th})$, can be calculated by using the dissipated electrical power at threshold in CW mode. At threshold, the temperature difference between the active region $T_{\rm act}$ and heat sink temperature $T_{\rm sink}$ is about 110 K from Fig. 4. With $I_{\rm th} =$ 1.5 A and $V_{\rm th} = 9.6$ V in CW operation at 270 K, the values of $R_{\rm th} = 7.64$ K/W [corresponding to the thermal conductance ($G_{\rm th} = 1/(R_{\rm th} A) = 300.9$ W/K·cm^2] is estimated using the above equation.

The coupling coefficient (κ) of the DFB grating can be estimated from the width of the stop band, which is observed from the CW the subthreshold spectrum at 140 K in Fig. 5. The inset is lasing spectrum of the device at the injection current of 0.32 A. For subthreshold current of $I = 0.318$ A, the stop band width is about 10.5 nm. The effective refractive index ($n_{\rm eff}$) is deduced from the Bragg wavelength $\lambda_{\rm B} = 2 n_{\rm eff} \Lambda$ and its value is 3.19 at 140 K. The coupling coefficient κ of the grating can also be determined from $\kappa = \Delta\lambda_0 \pi n_{\rm eff}/\lambda_{\rm B}^2$, where $\Delta\lambda_0$ is the stop band width[10]. We obtain the coupling coefficient $\kappa = 18.2$ cm^{-1}, which in turn yields $\kappa L \approx 5.46$ for a cavity length of 3 mm. This value is slightly higher than typically expected for optimum range (1–3), which suggests that the device is slightly overcoupled. As shown in the inset of Fig. 3, this overcoupling is helpful to secure single-mode operation at high operating currents.

4. Conclusion

In summary, we have demonstrated the CW performance of single-mode DFB-QCLs operating at $\lambda \approx 7.6$ μm up to temperatures of 280 K with SMSR about 30 dB. The holographic lithography technique is shown to be a very effective method to define DFB grating, which will be significant to the large-scale fabrication of DFB-QCLs.

Acknowledgement

The authors would like to thank P. Liang and Y. Hu for their help with the processing.

References

[1] Faist J, Gmachl C, Capasso F, et al. Distributed feedback quantum cascade lasers. Appl Phys Lett, 1997, 70: 2670
[2] Namjou K, Cai S, Whittaker E A, et al. Sensitive absorption spectroscopy with a room-temperature distributed-feedback quantum-cascade laser. Opt Lett, 1998, 23: 219
[3] Kosterev A, Tittel F. Chemical sensors based on quantum cascade lasers. IEEE J Quantum Electron, 2002, 38: 582
[4] Schrenk W, Finger N, Gianordoli S, et al. Surface-emitting distributed feedback quantum-cascade lasers. Appl Phys Lett, 2000, 77: 2086
[5] Bakhirkin Y A, Kosterev A A, Curl R F, et al. Sub-ppbv nitric oxide concentration measurements using CW thermoelectrically cooled quantum cascade laser-based integrated cavity output spectroscopy. Appl Phys B: Lasers Opt B, 2006, 82: 149
[6] Xie F, Caneau C G, LeBlanc H P, et al. High-temperature continuous wave operation of low power consumption single-mode distributed-feedback quantum-cascade lasers at $\lambda \sim 5.2$ μm. Appl Phys Lett, 2009, 95: 091110
[7] Lu Q Y, Bai Y, Bandyopadhyay N, et al. Room-temperature continuous wave operation of distributed feedback quantum cascade lasers with watt-level power output. Appl Phys Lett, 2010, 97: 231119
[8] Lu Q Y, Bai Y, Bandyopadhyay N, et al. 2.4 W room temperature continuous wave operation of distributed feedback quantum cascade lasers. Appl Phys Lett, 2011, 98: 181106
[9] Darvish S R, Slivken S, Evans A, et al. Room-temperature, high-power, and continuous-wave operation of distributed-feedback quantum cascade lasers at $\lambda \approx 9.6$ μm. Appl Phys Lett, 2006, 88: 201114
[10] Darvish S R, Zhang W, Evans A, et al. High-power, continuous-wave operation of distributed-feedback quantum-cascade lasers. Appl Phys Lett, 2006, 89: 251119
[11] Wittmann A, Bonetti Y, Fischer M, et al. Distributed-feedback quantum cascade lasers at 9 μm operating in continuous wave up to 423 K. IEEE Phototonics Technol Lett, 2009, 21: 12